TABLE OF CONTENTS

Appendix Supplementary Method

1. Generation of *dEsyt*^{KO} using CRISPR mediated deletion

Two sgRNAs were designed in the *dEsyt* genomic region, one sgRNA targeted the 5' end (approximately 250 bp downstream of the start codon, Target sequence: CCTCTCGGTGGCACGCGACCAGTTGG) and the second sgRNA targeted a region downstream of the second C2 domain in exon 12 (Target sequence: GCTGAAGCAATTCAATATGGAGG). The sites of the sgRNAs were chosen so as to not affect nearby genomic regions implicated in other processes (such as small nuclear RNA U6 gene and gene for tRNA Aspartic acid located near exon 13 of *dEsyt*). The resulting genome edit should remove 488 amino acids of the coding sequence from the 72nd amino acid in the splice variant PA and from the 105th amino acid in the splice variants PB, PC and PD of the *dEsyt* open reading frame which also includes the region encoding the SMP domain and the C2A domain (Appendix Figure S1A).

Transgenic flies expressing the dual gRNAs under the U6.2 promoter were crossed to *Act5c-Cas9* virgins. F1 progeny with a deletion of *dEsyt* gene was identified using a PCR based strategy obtaining DNA from heterozygotes at the F1 generation. Seven F1 progeny tested positive for this deletion; two with the brightest band (indicative of maximum number of cells with deletion) were further crossed to third chromosome balancers. 30 F2 progeny were screened for deletion and four of the pure lines were maintained as final heterozygous stocks, after confirming the absence of the dual gRNA and Cas9 transgenes. The genomic boundaries of the deletion were estimated by PCR based amplification with primers flanking the *dEsyt* genomic region. The mutant allele generated a band of 412 bp as against 3.7 kb region in controls (Appendix Figure S1C). Sanger sequencing of this PCR product was used to confirm the exact breakpoints (Appendix Figure S1B); this allele is referred to as *dEsyt*^{KO}.

dEsyt^{KO} was validated using RT-qPCR on total head RNA from homozygous flies- this showed negligible amounts of *dEsyt* transcripts in *dEsyt*^{KO} compared to controls (Appendix Figure S1D). Using an antibody against dEsyt for immunoblot analysis, *dEsyt*^{KO} was confirmed to be a protein null allele (Appendix Figure S1E). No change was detected in the transcript levels of the small nuclear RNA U6 gene (Appendix Figure S1F) and the genomic region of tRNA D96A (Appendix Figure S1G) in *dEsyt*^{KO}.

Appendix Figures

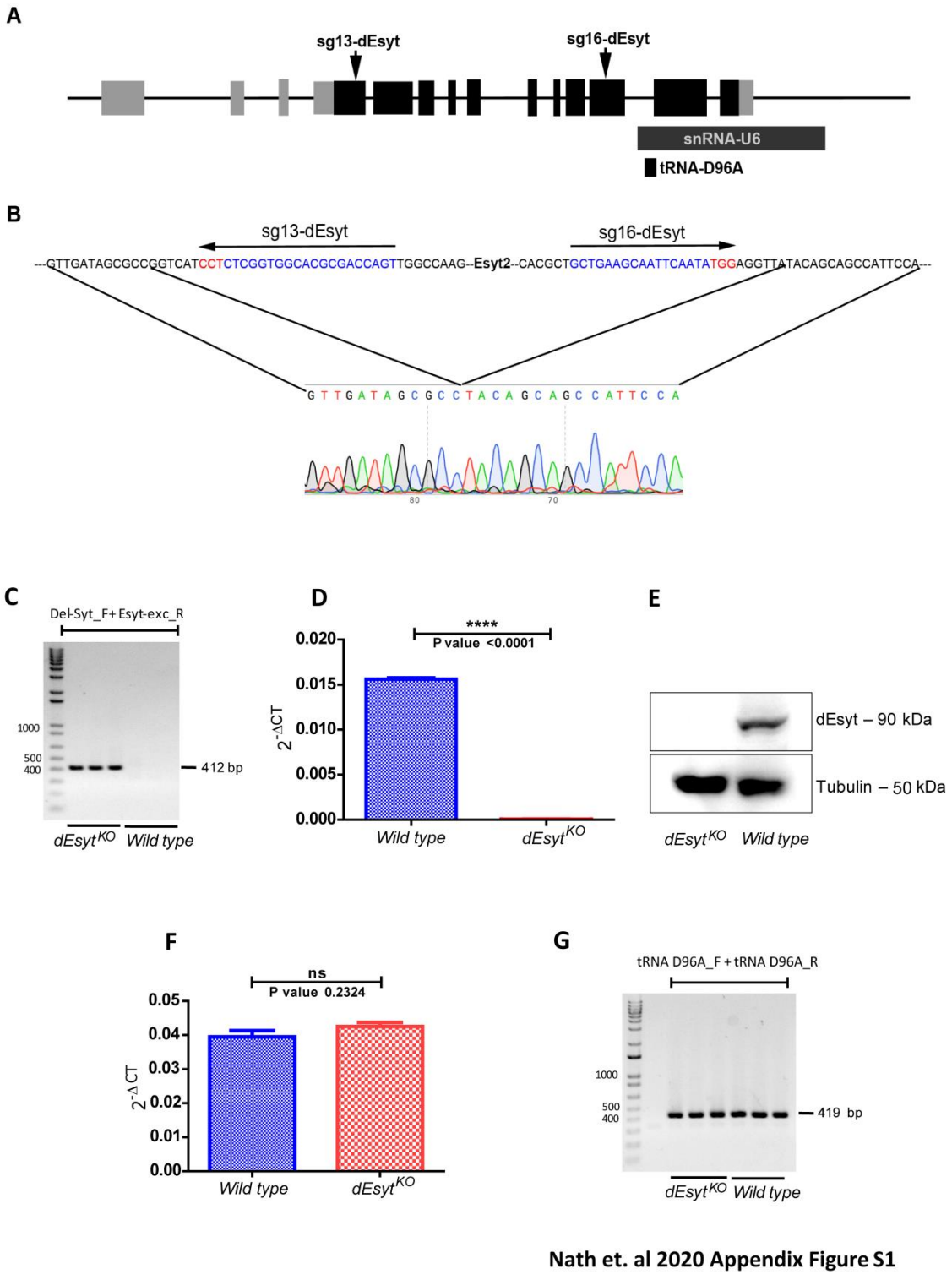

Nath et. al 2020 Appendix Figure S1

Appendix Figure S1: Generation of *dEsyt*^{KO} using CRISPR mediated deletion

(A) Schematic showing the position of sgRNAs designed to remove 488 aa from different splice variants of the *dEsyt* CDS using CRISPR mediated deletion. Intron/exon structure of

the *dEsyt* gene is shown. Coding exons are in black and non-coding exons in grey. Arrows indicate the position of the guide RNAs used in this study for genome engineering. snRNA-U6 and tRNA-D96A indicate the positions of these genes in relation to the *dEsyt* gene.

(B) Sanger sequencing chromatogram showing the precise breakpoints induced in the $dEsyt^{KO}$ allele used in this study. The DNA sequence is shown and the position of the guide RNAs is indicated.

(C) Image of agarose gel electrophoresis showing the PCR based verification of the knockout. A PCR amplification band of 412 bp is seen in the $dEsyt^{KO}$ but not in wild type. Primers used for the amplification are shown at the top of the gel and the size of fragments in the DNA ladder is shown in bp.

(D) Quantitative RT-PCR analysis showing *dEsyt* transcript level expression in the $dEsyt^{KO}$ and controls. Y-axis indicates the *dEsyt* transcript level expression normalized to the loading control (RP49- Ribosomal protein 49).

(E) Western blot from head extracts of the genotypes as indicated on the bottom of the blot. The blot was probed with antibody against dEsyt. Tubulin was used as the loading control.

(F) Comparative real time PCR analysis showing invariable transcript level expression in the small nuclear RNA U6 gene. X-axis shows genotypes and Y-axis indicates the *dEsyt* transcript level expression normalized to the loading control.

(E) A gel image showing the PCR based verification of the intact genomic region of tRNA D96A in the indicated genotypes. A band of 419 bp is seen in both wild type and $dEsyt^{KO}$.

Bar graphs with mean ± SD are shown. Statistical tests: (C and D) Students unpaired t test (two tailed). ns - p value > 0.05. ****p value <0.0001.

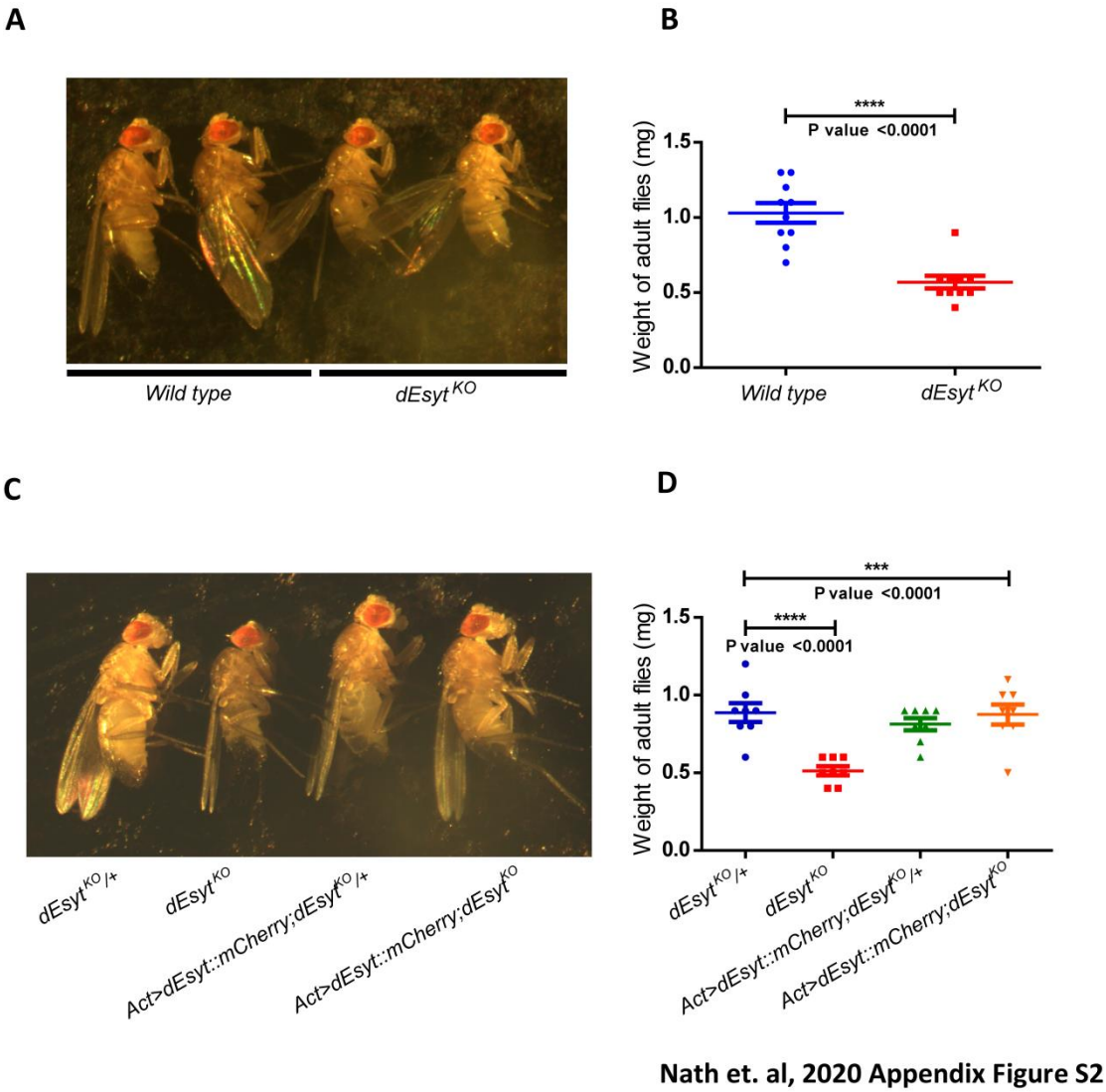

Appendix Figure S2: Reduced mass and body size in *dEsyt*^{KO} adults

(A) Representative image of adult flies showing the reduced body size in *dEsyt* knockout mutants.

(B) Quantification of the reduced mass of *dEsyt*^{KO} v Wild type. n=10 flies.

(C) Representative image showing the rescue of body size by the transgenic expression of dEsyt::mCherry in *dEsyt*^{KO} homozygotes.

(D) Quantification of the rescue in body mass of flies shown in image C. n=10 flies

Scatter plots with mean ± SD are shown. Statistical tests: (B) Student's unpaired t test. (D) one-way ANOVA with post hoc Tukey's multiple pairwise comparison. ***p value <0.001; ****p value <0.0001.

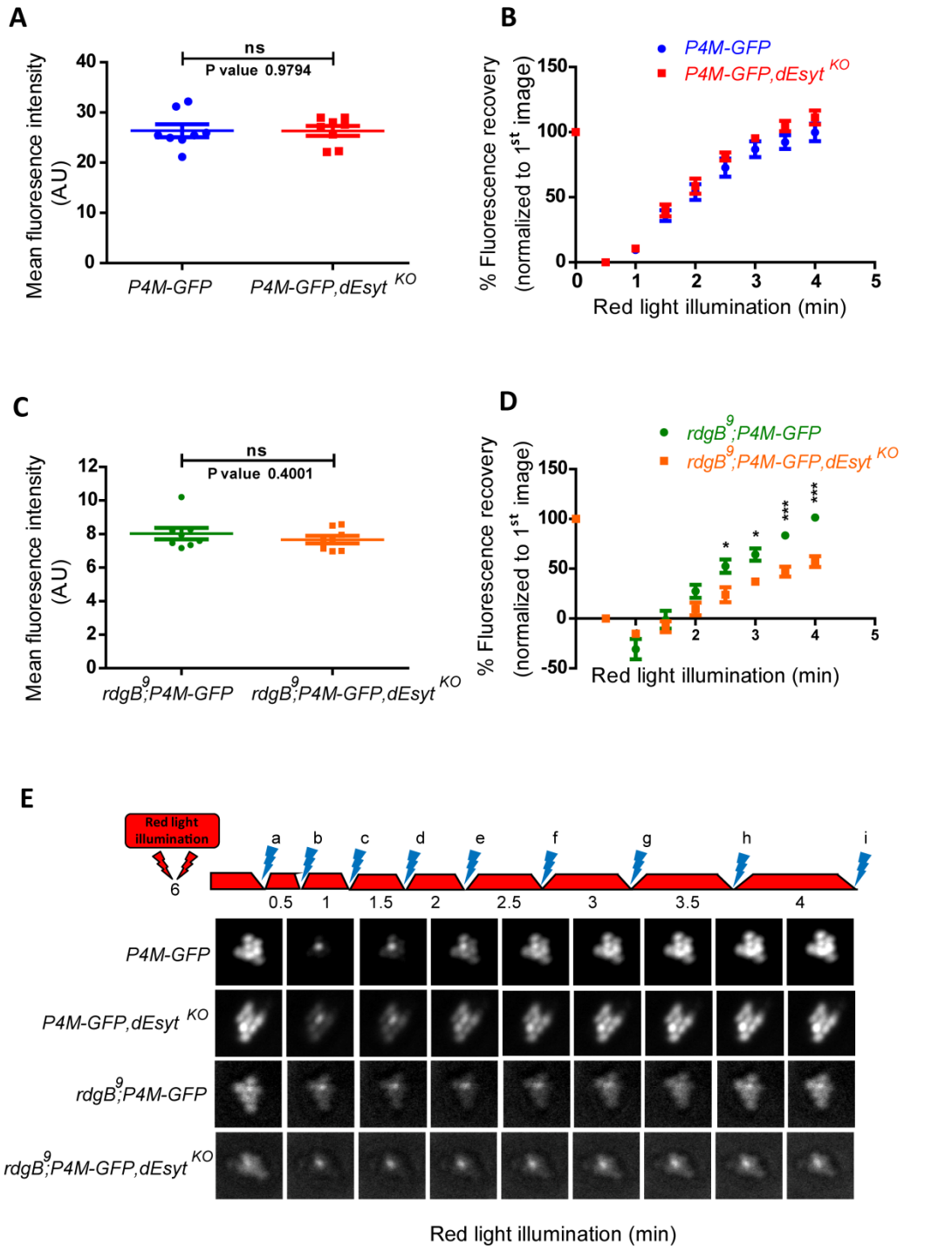

Nath et. al, 2020 Appendix Figure S3

Appendix Figure S3: Loss of *dEsyt* delays the PI4P recovery kinetics in *rdgB*^{9}

(A,C) Quantification of the mean fluorescence intensity of the deep pseudopupil formed by the PI4P probe P4M-GFP in one day old flies of the indicated genotypes (n=8).

(B,D) Graph showing the recovery kinetics of the fluorescent pseudopupil with time, X-axis represent the genotypes, Y-axis represent intensity expressed as percentage intensity of each pseudopupil acquired at different time points normalized to the intensity of the first image acquired (n=8).

(E) Representative deep pseudopupil images from one day old flies expressing P4M-GFP probe acquired at specified time points. Genotypes as indicated (n=8).

Scatter plots and XY plots with mean ± SD are shown. Statistical tests: (A and C) Student's unpaired t test. (B and D) Two-Way ANOVA Grouped analysis with Bonferroni post-tests to compare replicate means. ns - p value > 0.05; **p value < 0.01; ***p value < 0.001; ****p value <0.0001.

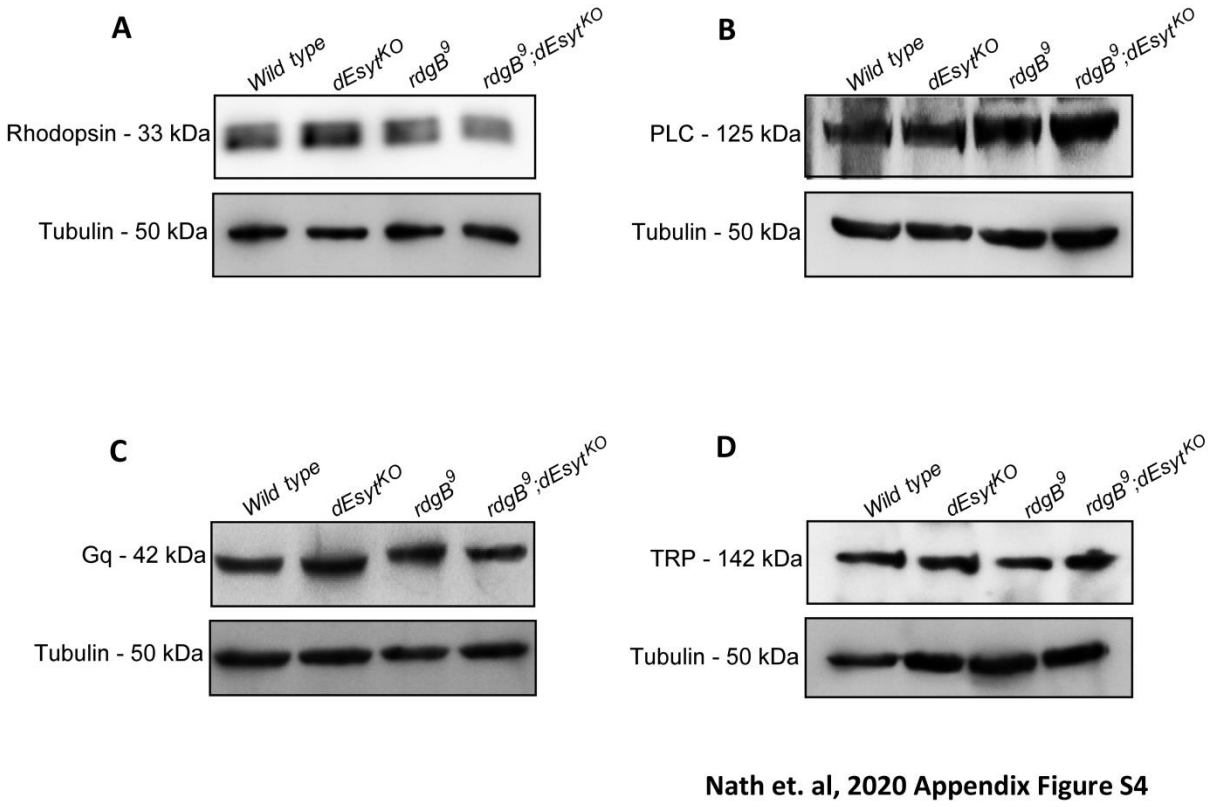

Appendix Figure S4: Loss of *dEsyt* does not affect the levels of key phototransduction proteins in *rdgB*^{9}

Western blot of head extracts made from flies of the indicated genotypes. Tubulin was used as the loading control for the experiment. The blots were probed for the major phototransduction proteins:

(A) Rhodopsin

(B) Gq

(C) PLC

(D) TRP

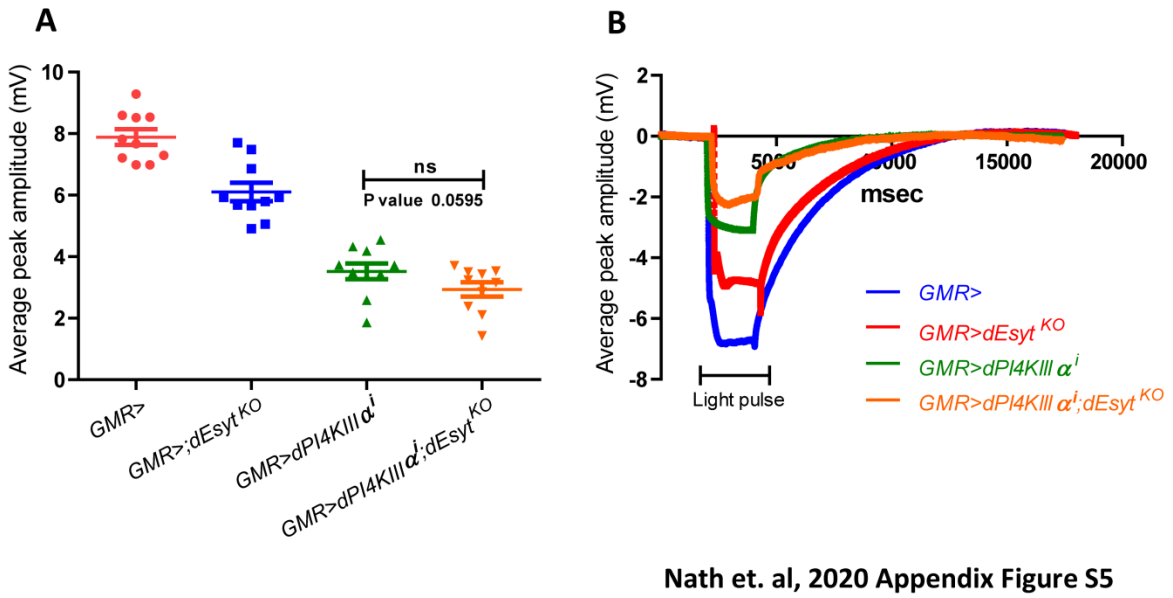

Appendix Figure S5: ERG amplitude remains unaffected in *dEsyt* knocked out *PI4KIIIα* mutants

(A) Average ERG response of 0-1 day dark reared flies of the indicated genotype to a 2s flash of green light; n=10.

(B) Representative traces of ERG showing the duration of light pulse, X-axis indicates time in msec and Y-axis indicates the average ERG amplitude in mV.

Scatter plots with mean ± SD are shown. Statistical tests: (A) one-way ANOVA with post hoc Tukey's multiple pairwise comparison. ns - p value > 0.05.

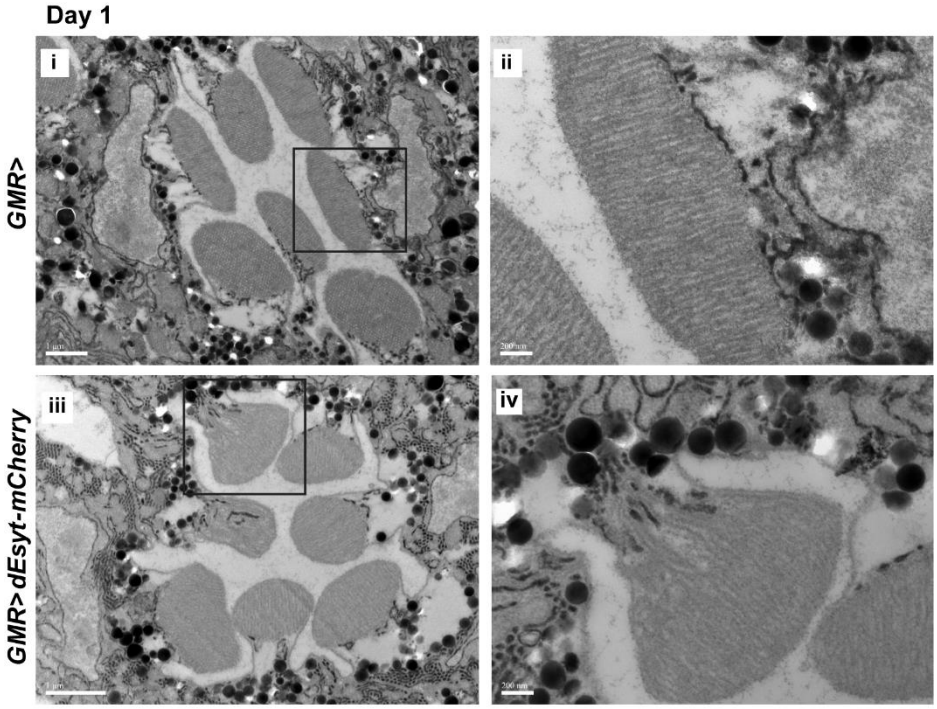

Nath et. al, 2020 Appendix Figure S6

Appendix Figure S6: Overexpression of dEsyt recruits ER structures towards the rhabdomere

TEM images of a single ommatidium from photoreceptors of flies, in which dEsyt::mcherry is exogenously expressed using an eye specific promoter GMR-Gal4, reared in dark, scale bar: 1 µM. GMR-Gal4 is shown as control **(A) (i)** *GMR-Gal4-* day 1 **(iii)** *GMR-Gal4>dEsyt::mcherry-* day 14 **(A-ii, iv)** Magnified image showing a single photoreceptor from the ommatidium image shown on the left. Scale bar: 200 nm. Origin boxes for magnification shown.